ISSN: 1410-8917
e-ISSN: 2597-9914

Jurnal Kimia Sains dan Aplikasi 27 (5) (2024): 197-204

Jurnal Kimia Sains dan Aplikasi
Journal of Scientific and Applied Chemistry

Journal homepage: http://ejournal.undip.ac.id/index.php/ksa

Na_2SO_3 Salt Effect on The Ionic Conductivity of Solid Polymer Electrolyte (SPE) Based on Polyvinyl Alcohol

Sylvia Ayu Pradanawati [1,*], Albert Turnip [1], Nur Laila Hamidah [2], Yose Fachmi Buys [1]

[1] Department of Mechanical Engineering, Faculty of Industrial Technology, Universitas Pertamina, Jakarta, Indonesia
[2] Department of Engineering Physics, Institut Teknologi Sepuluh Nopember, Kampus ITS Sukolilo, Surabaya 60111, Indonesia

* Corresponding author: sylvia.pradanawati@universitaspertamina.ac.id

https://doi.org/10.14710/jksa.27.5.197-204

Article Info

Article history:

Received: 12th February 2024
Revised: 02nd April 2024
Accepted: 28th April 2024
Online: 31st May 2024

Keywords:
Solid Polymer electrolyte (SPE); Polyvinyl Alcohol (PVA); Sodium Sulfite; amorphous; Ionic Conductivity

Abstract

This research is about solid polymer electrolyte (SPE) based on polyvinyl alcohol (PVA) synthesized using a solution casting technique by adding variations of sodium sulfite salt and glycerol as fillers to reduce the samples' bulk resistance for electrochemical energy storage application. The method used is a quantitative analysis based on the test results. X-ray Diffraction (XRD) was used to determine the crystallinity and structure of the solid polymer electrolyte material. Interactions between Na^+ ions from salts in SPE were analyzed using Fourier transform infrared (FTIR). The mechanical properties of the SPE samples were analyzed using tensile testing (ultimate tensile strength). Solid polymer electrolyte (SPE) ion conductivity was analyzed using electrochemical impedance spectroscopy (EIS) with temperature variations of 25, 40, 50, 60, and 70°C. The maximum SPE ionic conductivity value is 1.05×10^{-5} S cm^{-1} in a PVA-Glycerol-Na_2SO_3 15% sample at 70°C.

1. Introduction

The level of energy consumption is impacted by the expanding human population [1]. In Indonesia, the primary energy source is still the usage of fossil fuels, particularly coal and oil [2]. In 2018, 311.6 MTOE of primary energy total was produced, including fossil and New and Renewable Energy. Liquefied natural gas (LNG) and coal exports account for 64% of the total Total Primary energy Production (TPEP). Moreover, Indonesia imported 43.2 MTOE of crude oil to be utilized in fuel oil production. The transportation sector accounts for 40% of Indonesia's energy use, followed by the industrial sector, which uses 36%; the household sector, which uses 16%; the commercial sector, which uses 6%; and other sectors, which use 2% [3]. The availability of fossil energy is decreasing due to large-scale fossil energy exploration.

Furthermore, New Renewable Energy (NRE) is implemented as a fossil fuel availability solution. Increasing the use of NRE is accomplished by utilizing all available natural resources, such as rivers, sunlight, and wind. Hydroelectric power plants, solar power plants, wind power plants, and other power plants with renewable energy sources are examples of New and Renewable Energy Plants (NREP). The Indonesian government is expected to seek new and renewable energy sources to reduce the use of fossil fuels and be environmentally friendly [4]. Indonesia's NRE target for the national energy mix in the year 2025 is 25%. As quoted from the secretariat of the cabinet of the Republic of Indonesia this is done to meet Indonesia's commitment to reduce emissions by up to 29% by 2030 and achieve a clear goal of a cleaner and more sustainable energy system. Aside from the large sources of new renewable energy, one of the weaknesses of new renewable energy is its intermittent nature. The intermittent characteristic denotes the lack of consistent availability of NRE at the required moment.

Energy storage technology is required to overcome the shortcomings of renewable energy. Energy storage systems comprise a variety of technologies and processes for storing mechanical, thermal, electrical, electrochemical, chemical, wind, and solar energy, among others [5]. Electrochemical storage, which includes capacitors, batteries, and supercapacitors, is the most used type of energy storage. Electrodes and

electrolytes are two of the main components of the energy storage system. The electrodes are positive (cathode) and negative (anode), and the electrolytes are liquid and solid.

Polymer electrolytes are solid substances composed of elongated molecular chains known as polymers. Polymers that can conduct ions are known as electrolyte polymers, and this property makes them useful as building blocks for the creation of electrolytes. The purpose of these polymers is to incorporate ions that possess the ability to traverse their structure, hence enabling the transportation of ions during electrochemical reactions [6]. In contrast to liquid electrolytes, which possess the ability to flow and potentially experience leakage, polymer electrolytes exhibit stability and resistance to leakage owing to their solid state [7]. The ion conduction mechanism in polymer electrolytes entails the movement of ions through the polymer matrix through diffusion.

In the electrochemical device, the movement of ions occurs between the positive and negative electrodes, facilitating the generation of an electric current. The regulated diffusion mechanism facilitates efficient ion transfer while mitigating the potential dangers associated with liquid electrolytes. For electrochemical storage devices, polymer electrolytes offer a safer and more stable alternative to liquid electrolytes [8]. Their solid composition, combined with strong ionic conductivity and controlled ion diffusion, makes them essential components for modern energy storage technologies.

The mechanical characteristics of solid polymer electrolytes, specifically their flexibility, have an impact on their ionic conductivity [9]. The ions present in SPE are mobilized differently depending on the elasticity of SPE. Because of the SPE's more amorphous crystal structure, ion transport is made easier the more elastic the SPE is produced. SPE's amorphous crystal structure makes the cavities wider, allowing ions to move more freely and smoothly. In order to determine the mechanical characteristics of the SPE, a tensile test is required. The polymer polyvinyl alcohol (PVA) can be used as a polymer electrolyte [10, 11]. PVA is suited for usage as an electrolyte for green energy due to its hydrophilic and biodegradable characteristics [12].

The solid polymer electrolyte necessitates the addition of salt to enhance its ionic conductivity, while glycerol serves as a plasticizer to enhance the elasticity of the polymer's structure [13, 14]. This, in turn, facilitates the transit of electrons, resulting in an increase in ionic conductivity up to 7.5×10^{-4} S cm^{-1} [15]. The objective of this study is to enhance the conductivity of polymer electrolytes based on polyvinyl alcohol (PVA) and glycerol by incorporating Na_2SO_3 salts, which are recognized for their exceptional compound stability and capacity to improve anodic current density [16].

2. Experimental

2.1. Materials

The materials employed in this study were polyvinyl alcohol (PVA), a water-soluble polymer obtained from Sigma Aldrich, glycerol (Himedia, 85%), sodium sulfite (Na_2SO_3) (Anhydrate, Pudak Scientific), and distilled water.

2.2. Synthesis Stage

Afterward, all the tools were cleaned with 96% ethanol to remove any contaminants after preparing the instruments and supplies. A 50 mL measuring cup was prepared, followed by the addition of 50 mL of distilled water. Subsequently, the cup was subjected to heat until it reached a temperature of 90°C. The subsequent procedure involved the addition of 1 gram of PVA and Na_2SO_3 salt to the solution, with increments of 0, 0.05, 0.1, 0.15, and 0.2 grams. After that, a hot plate was used to stir the mixture until it was homogeneous. While the solution reached homogeneity, 0.5 grams of glycerol were introduced. The quantity of glycerol was carefully adjusted to achieve the optimal composition, serving several purposes: it acted as a plasticizer, enhanced ionic conductivity, adjusted viscosity, and provided beneficial solvent properties. The temperature was then reduced to room temperature and stirred for 24 hours. The solution was poured onto the petri dish using the Teflon casting method and dried in the oven for 12 hours prior to use.

2.3. Testing Stage

Both characterization testing and performance tests were run as part of this investigation. The performance testing was carried out utilizing electrochemical impedance spectroscopy (EIS) with the AutoLab system and tensile tests with the ZwickRoell. Each sample underwent three runs of the performance test for each type of test conducted on the samples. The ionic conductivity value of the sample was calculated by measuring its resistance on the Nyquist plot analysis. Meanwhile, the Ultimate Testing Machine (UTM) was used for tensile testing. When conducting ionic conductivity tests for polymers, it is essential to maintain operating conditions that support environmental humidity. This is because humidity can significantly influence the conductivity values of materials by affecting ion mobility and potentially causing polymer degradation [17]. A glove box and desiccator were utilized for storage and a crimped cell was employed for testing to prevent moisture from entering throughout the experiment.

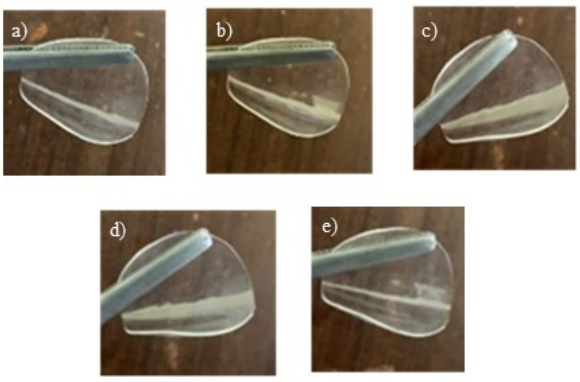

Figure 1. The physical observation of the PVA and glycerol synthesis with different amounts of Na_2SO_3 added (a) 0%, (b) 5%, (c) 10%, (d) 15%, and (e) 20%

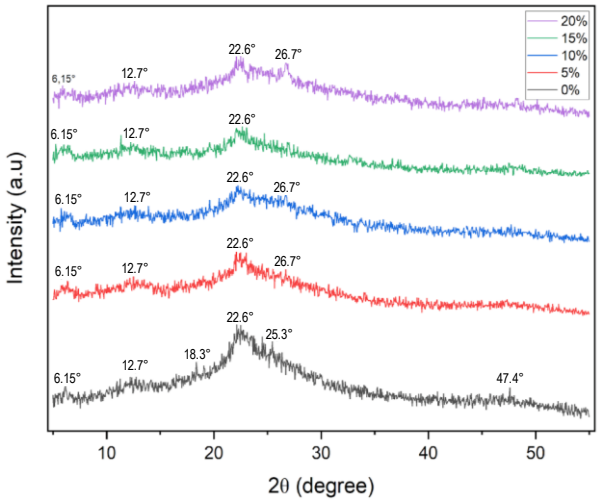

Figure 2. The XRD diffractogram of the PVA-Glycerol/Na_2SO_3 film with salt and pure SPE added

For the parameters and equipment used during the analysis, Fourier Transform Infrared (FTIR) spectroscopy measurements were conducted using a Thermo Scientific Nicolet iS5 spectrophotometer equipped with an ATR iD7 accessory. The measurements were taken over a wavenumber range of 4000 to 400 cm^{-1}. X-ray diffraction (XRD) patterns were recorded using Olympus BTX-534 with Cu-Kα for 2θ measurements ranging from 5° to 90°. Fourier Transform Infrared (FTIR) spectroscopy, a powerful analytical technique, was employed to identify functional groups in molecules based on their absorption of infrared radiation.

3. Results and Discussion

3.1. SPE Synthesis Results

Solution casting is a synthetic technique used to create solid polymer electrolytes (SPEs). In this process, the host polymer, additives, salts (ionic dopants), and solvents that constitute an SPE were mixed and gelatinized. The resulting mixture was then cast into petri dishes to form the final product. PVA serves as the host polymer, glycerol as an additive, sodium sulfite salt as an ionic dopant, and distilled water as the solvent. In this investigation, the salt ratio in every sample was considered when modifying the SPE. SPE's ionic conductivity is improved by the salt. There were five different ways to apply salt: 0, 0.05, 0.1, 0.15, and 0.2 g. To hydrolyze the Na_2SO_3 salt and produce Na^+ and SO_3^{2-} ions, the polymer and salt must be dissolved in distilled water at 90°C until homogenous.

Table 1. FWHM value calculation results on SPE variations

PVA-Glycerol-Na_2SO_3 (%)	FWHM
0	11.981
5	21.494
10	22.647
15	27.440
20	20.988

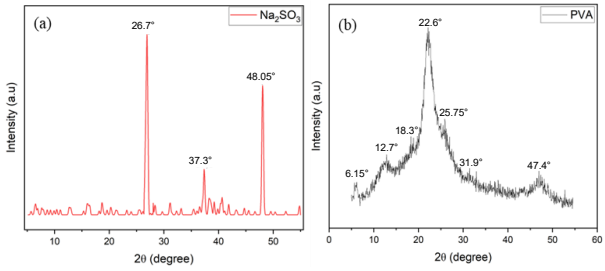

Figure 3. The XRD diffractograms of (a) Na_2SO_3 salt and (b) PVA

After becoming homogeneous, the solution's temperature was decreased to room temperature, and the glycerol was added dan stirred for 24 hours. The gelatinization process was carried out using a hotplate. A homogenous solution was created in a petri dish with a 90 mm diameter and 15 mm side height. SPE films were then created by drying the SPE solution for 12 hours at 50°C. Before testing was done, the produced film was then placed in a plastic clip for storage. According to the results of the synthesis, the amount of salt added had an impact on the physical characteristics of SPE. With more salt applied, SPE film becomes more fragile and less elastic [18]. There is no visible color shift on the SPE film for all samples with varying salt variations (Figure 1). Further effects of salt addition on the SPE film were investigated through characterization and performance tests in the following stage.

3.2. XRD Test Results

SPE sample variations in crystal structure were examined using XRD. The interaction between the PVA polymer and salt causes changes in the crystal structure of the SPE. The ionic conductivity of the sample is influenced by its crystal structure, with higher levels of amorphousness correlating to increased ionic conductivity [19]. XRD analysis was performed on SPE, PVA, and Na_2SO_3 salt. Figure 2 presents the findings of the XRD characterization test. Diffraction graphs for the SPE, salt, and PVA polymer samples demonstrate distinct discrepancies in the test results. Specifically, the largest diffraction peaks for the Na_2SO_3 salt were observed at 2θ = 26.7°, 37.3°, and 48.05°. In contrast, diffraction peaks for pure PVA polymer were found at 2θ = 6.15°, 12.7°, 18.3°, 22.6°, 25.75°, 31.9°, and 47.4°.

Compared to pure PVA polymer powder, SPE film made from PVA polymer exhibits a lower diffraction peak. This demonstrates that the manufactured SPE film samples are amorphous. The PVA polymer's crystal structure finally transformed into an amorphous state due to the release of the OH chain and the viscosity rising during the gelatination process. The crystal structure of SPE changes due to the addition of the Na_2SO_3 salt. This discrepancy in diffraction peaks between pure PVA and PVA-Glycerol-Na_2SO_3 is illustrated in Figure 3. Pure PVA polymer has a diffraction peak at 2θ = 31.9°; however, the PVA-Glycerol-Na_2SO_3 sample lacks a diffraction peak at that corner. In the PVA-Glycerol-Na_2SO_3 sample with changes of salt above 0%, the peak expands at 2θ = 18.3°, 25.75°, and 47.4°, demonstrating the difference at those angles.

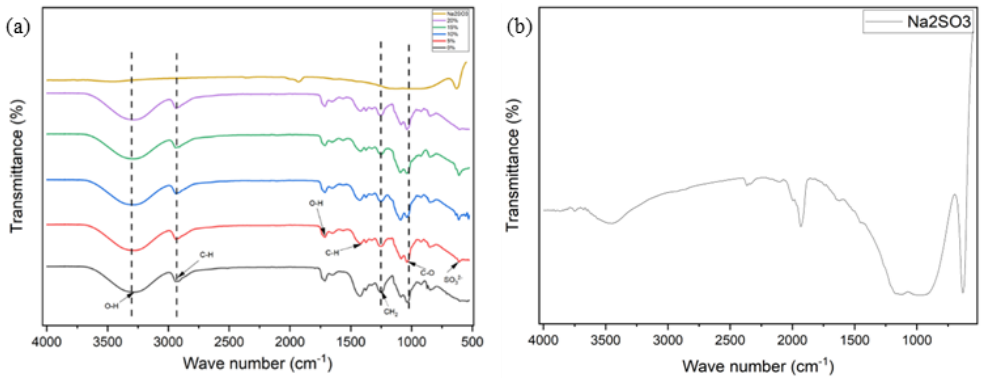

Figure 4. FTIR spectra of (a) PVA-Glycerol-Na_2SO_3 with various amounts of salts (b) Na_2SO_3 enlargement

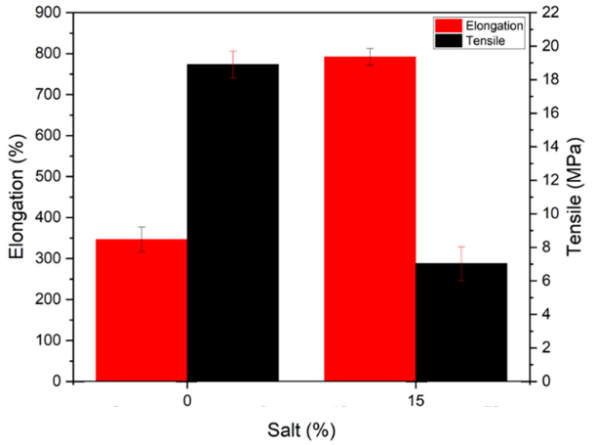

Figure 5. Graph of tensile strength and elongation test of PVA-Glycerol-Na_2SO_3 with variations of 0% and 15% salt

The release of the OH chain during the SPE synthesis process was responsible for broadening the diffraction peaks. The crystal structure of the 0% PVA-Glycerol-Na_2SO_3 SPE sample was altered by the addition of the Na_2SO_3 salt. Changes in crystal structure are located at angles 2θ = 18.3°, 25.75°, and 47.4°, indicating the presence of diffraction peaks in the 0% PVA-Glycerol-Na_2SO_3 samples. However, diffraction peaks at these angles are absent in 5% PVA-Glycerol-Na_2SO_3, PVA-Glycerol-Na_2SO_3 10%, PVA-Glycerol-Na_2SO_3 15%, PVA-Glycerol-Na_2SO_3 20%. These modifications show that salt makes the SPE structure more amorphous [20, 21].

Utilizing the OriginLab application to measure the full-width half maximum (FWHM) value revealed significant differences attributable to variations in salt content across samples. As the amount of salt increased, the FWHM value also increased, reaching a maximum of 27.439 in the 15% PVA-Glycerol-Na_2SO_3 sample. This trend indicates that the SPE sample adopts a more amorphous phase with enhanced conductivity, ductility, and stability. These characteristics are reflected in a larger FWHM value and lower crystallinity. The increment of the amorphous phase led to increasing ionic conductivity due to the relaxation of the matrix polymer and allowed ion movement easier [22]. Nevertheless, the FWHM value exhibited a decline in the 20% sample, primarily due to the increase of crystallization degree by salt addition. This occurred because the host polymer in the SPE sample was unable to accommodate the additional salt [23].

3.3. FTIR Test Results

The functional groups present in the SPE sample were identified using FTIR testing. A test is conducted to determine whether the addition of Na_2SO_3 salt to the SPE sample results in the formation of new functional groups or the loss of existing ones due to the breaking and forming of chemical bonds. A spectrum graph displaying changes in transmittance for each infrared radiation wave represents the findings of the FTIR characterization test [24, 25]. The FTIR test results in this investigation revealed an infrared spectrum with wavelengths ranging from 600 cm^{-1} to 4000 cm^{-1}. The spectrum produced in this study was compared with reference research and compound spectrum correlation tables to ensure the presence of functional groups in the FTIR test results. Figure 4 displays the FTIR spectra of this study's result.

The remaining O-H and C-H bond region (between 2500 and 4000 cm^{-1}), the double bond region (1500 and 2000 cm^{-1}), the triple bond region (between 2000 and 2500 cm^{-1}), and the fingerprint region (between 600 and 1500 cm^{-1}) are the four regions that make up the FTIR spectra. The O-H stretching functional group is detected as having a broad absorption region at wavenumber 3291 cm^{-1} in the spectrum of sample 0% absorbing region. This absorption falls within the single bond region, encompassing all such bonds. The asymmetrically stretched C-H functional group has an absorption region at wavenumber 2917 cm^{-1}. No functional group absorption zones exist in the triple bond region, which has wavenumbers between 2000 and 2500 cm^{-1}. This demonstrates that functional groups with triple bonds are absent in the SPE synthesis's final products.

Additionally, the FTIR peaks in this region exhibit a shifting pattern when Na_2SO_3 is combined with PVA as a composite. The observed shifting could potentially signify a hydrogen bonding interaction between the polymer matrix and salt, as polyvinyl alcohol is a repeating unit polymer that contains hydroxyl (-OH) groups that establish hydrogen bonds. Several functional group absorption regions were identified in the fingerprint area of the spectrum. These include the bending vibration of the CH_2 functional group at a wavenumber of 1248 cm^{-1} and the stretching vibration of C-H at a wavenumber of 1437 cm^{-1}, originating from CH_2 in the PVA backbone. Additionally, stretching vibrations of C-O were observed at a wavenumber of 1035 cm^{-1}, characteristic of PVA polymers.

Table 2. Ionic conductivity value at elevated temperature

PVA-Gliserol-Na_2SO_3 (%)	Ionic conductivity (S cm^{-1})				
	25°C	40°C	50°C	60°C	70°C
0	1.35×10^{-6}	1.57×10^{-6}	2.14×10^{-6}	4.01×10^{-6}	4.34×10^{-6}
5	1.03×10^{-5}	1.09×10^{-5}	1.14×10^{-5}	1.58×10^{-5}	1.79×10^{-5}
10	1.93×10^{-5}	2.39×10^{-5}	2.50×10^{-5}	3.58×10^{-5}	4.15×10^{-5}
15	3.45×10^{-5}	3.91×10^{-5}	4.22×10^{-5}	4.71×10^{-5}	1.05×10^{-4}
20	2.35×10^{-5}	2.94×10^{-5}	3.23×10^{-5}	3.88×10^{-5}	6.36×10^{-5}

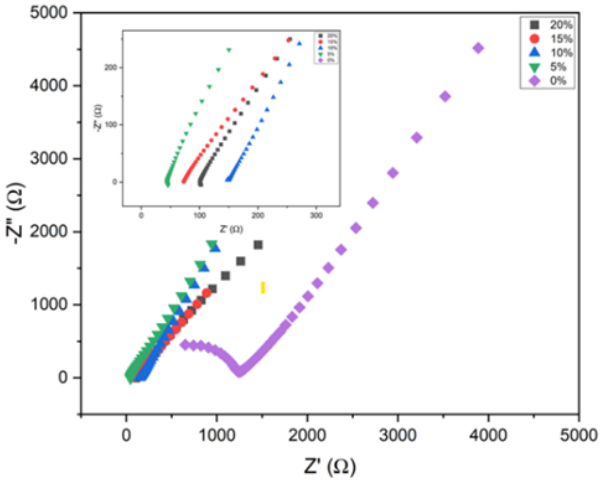

Figure 6. Nyquist plot of PVA-Glycerol-Na_2SO_3 samples at room temperature (25°C)

Furthermore, an absorption region at a wavenumber of 611 cm^{-1} was noted in samples containing salt, attributed to the SO_3^{2-} functional group from the salt compound. From these results, it is evident that the addition of salt alters the functional groups compared to the 0% sample. The degradation of the magnitude of the crystalline band in the region of 1437 cm^{-1} suggests that the CH_2 functional group is weakening due to the salt addition. This observation is further supported by the XRD results, indicating that weakening the CH_2 bond in PVA leads to the degradation of crystallinity in the sample.

3.4. Tensile Strength Results

The SPE samples in this investigation were evaluated three times for the most and the least amorphous SPE variations. The 15% PVA-Glycerol-Na_2SO_3 sample was identified as the most amorphous SPE variation, whereas the 0% PVA-Glycerol-Na_2SO_3 sample was considered the least amorphous. The tensile test chart and the elongation chart are then updated with the average value of the test results. The difference between the samples for each SPE modification in Figure 5 highlights the relationship between the material's UTS and elongation value. The amount of salt added to the SPE sample significantly impacts both the UTS value and its elongation: as more salt is added, the UTS decreases. Conversely, the elongation value increases with the addition of salt, exhibiting an inverse correlation with UTS. For instance, when salt was introduced to the 15% PVA-Glycerol-Na_2SO_3 sample, the UTS value decreased from 18.9 MPa in the 0% PVA-Glycerol-Na_2SO_3 sample to 7.033 MPa. Meanwhile, the elongation value increased from 346.5% for the 0% PVA-Glycerol-Na_2SO_3 sample to 792.1% for the 15% PVA-Glycerol-Na_2SO_3 sample with the addition of salt.

These results show that Na_2SO_3 plays a crucial role in altering the mechanical properties of the sample, particularly the UTS and elongation values. The increased salt concentration resulted in a notable reduction in UTS, while also raising the elongation value. This can be attributed to the higher degree of crystallinity in the XRD data. The increment in crystallinity degree observed in the XRD data suggests that the higher concentration of salt promotes more ordered packing of polymer chains that contribute to stronger polymer chain interaction [26].

3.5. EIS Test Results

The analytical emphasis of this test is directed towards the determination of bulk resistance values derived from the Nyquist plot generated by the Nova application. A graph known as the Nyquist plot displays impedance value data (Z), which is made up of real impedance (Z') and imaginary impedance (Z''). Figure 6 shows the Nyquist pattern obtained from EIS testing for all samples at room temperature, with frequencies ranging from 10 Hz to 10^6 Hz. Semicircle curves and linear curves can be seen in the Nyquist plot findings. A high frequency can be found in the semicircle curve shown in Figure 6. This suggests that there has been an ion transfer. Conversely, the linear curve in Figure 6 indicates a diffusion process at low frequency. The 0% PVA-Glycerol-Na_2SO_3 sample has the greatest semicircle curve in the illustration.

Meanwhile, the semicircle curve is substantially smaller in PVA-Glycerol-Na_2SO_3 with salt addition. A slower ion transport is shown by a wider resultant semicircle curve, which also implies a higher resistance value. The semicircle curve formed in the PVA-Glycerol-Na_2SO_3 sample with salt addition is significantly smaller than the semicircle curve formed in the PVA-Glycerol-Na_2SO_3 sample without salt addition. This demonstrates that adding salt to the sample significantly reduces its resistance. The distance on the impedance axis (Z') between the semicircle curve's first and final intersections is known as bulk resistance (R_b). The R_b value was calculated using the Nova application's circle fit approach, t and A correlate with thickness and area,

respectively, and the ionic conductivity value was calculated using Equation (1).

$$\sigma = \frac{t}{A \times R_b} \quad (1)$$

Table 2 shows that the sample containing 0% PVA, glycerol, and Na_2SO_3 had the highest bulk resistance, with an ionic conductivity of 1.35×10^{-6} S cm^{-1}. After the addition of Na_2SO_3 salt, the resistivity of the sample decreased. The interplay of Na^+ ions from the polymer's salts and an increase in ionic conductivity causes a reduction in resistance. In SPE, the Na^+ cation has a weak interaction with O^-, allowing it to migrate freely from one open site to the next to create an ionic conduction mechanism [27, 28]. The ionic conductivity value increases as the salt content in SPE increases because more ions are concentrated in the SPE matrix [21, 29].

The 15% PVA-Glycerol-Na_2SO_3 sample, according to the testing results, has the lowest bulk resistance value of 1840.915 Ω and the highest ionic conductivity value of 3.45×10^{-5} S cm^{-1} at room temperature. After 20% salt addition, the ionic conductivity significantly drops due to the salt concentration being overcrowded in the polymer matrix so that ion mobility decreases [29]. The ionic conductivity of the sample progressively falls due to the reduction in ion mobility. Based on the XRD data, 20% salt addition, the crystallinity is increased and leads to a reduction in the ionic conductivity. At a certain amount of salt, the salt could act as a diluent for the polymer chain. After the optimum condition, excessive salt addition can lead to the agglomeration of salt particles, creating barriers within the polymer matrix that restrict the movement of ions.

In this work, EIS testing was done at high temperatures to observe how the materials' ionic conductivity values changed as the temperature rose. According to Table 2, at a temperature of 70°C, the sample 15% had the highest conductivity value, with an ionic conductivity value of 1.05×10^{-5} S cm^{-1}. Figure 7 depicts the trend of conductivity values changing as the temperature changes. Figure 7 illustrates the changes in ionic conductivity as temperature increases. The graph clearly shows a direct correlation between rising temperature and increasing ionic conductivity. As the temperature of the SPE increases, its resistance decreases. This phenomenon occurs because the bonds between Na^+ and O^- ions are more easily loosened at higher temperatures, thereby enhancing ion mobility.

The Arrhenius model can be used to study the rise in ionic conductivity that is influenced by variations in temperature. The link between ionic conductivity and activation energy is explained by Arrhenius modeling (E_a). Using the Arrhenius equation, it is possible to determine the activation energy (Equation (1)), the slope can be calculated through linear fit from Equation (2) from $-E_a$ divided by R.

$$ln\ \sigma = \frac{-E_a}{RT} + \ln A \quad (2)$$

Equations (1) and (2) show that the sample's ionic conductivity value is inversely proportional to the activation energy level. Ionic conductivity values decrease as activation energy increases and vice versa. Obtaining the activation energy value involves analyzing the slope (gradient) of the log plot for ionic conductivity with respect to 1000/T.

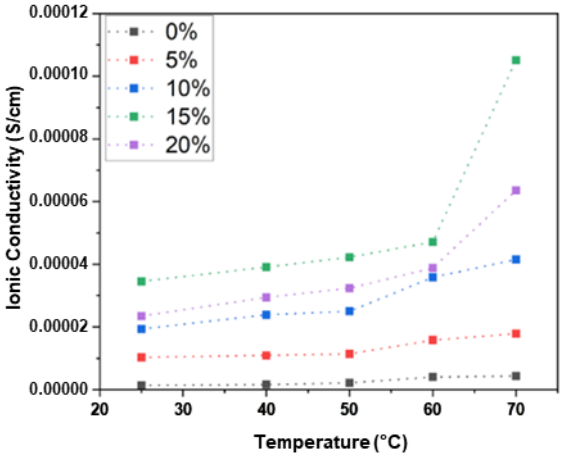

Figure 7. The trend of change in ionic conductivity at elevated temperatures

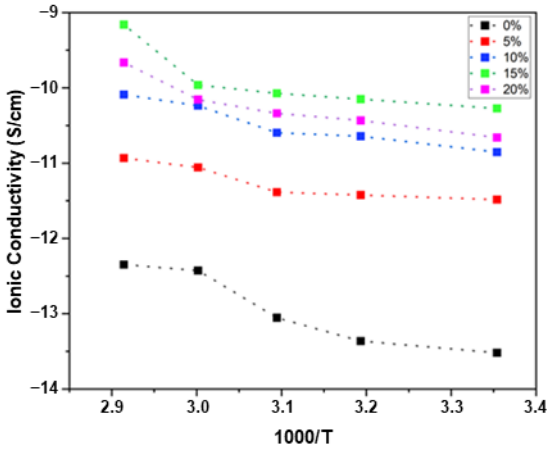

Figure 8. The link between the inverse temperature of 1000/T and the logarithm of ionic conductivity (K^{-1})

Table 3. Energy activation for the PVA-Glycerol-Na_2SO_3 sample

PVA-Gliserol-Na_2SO_3 (%)	Gradient	E_a (J/mol)
0	-2.965	24.645
5	-2.116	17.591
10	-2.047	17.017
15	-1.306	10.860
20	-1.761	14.641

Activation energy refers to the amount of energy required to break bonds in chemical compounds and create new ones. The capacity of ions to exit and migrate inside the polymer matrix is intricately linked to this phenomenon. Table 3 indicates a decreasing trend in activation energy because of salt addition. The observed decrease in activation energy indicates that ion transfer is characterized by rapid and facile occurrence. Moreover, the reduced energy activation condition facilitates the facile migration of the Na^+ ion within the polymer matrix [30].

4. Conclusion

The crystal structure of polyvinyl alcohol (PVA) becomes amorphous when SPE is synthesized from it. The SPE sample with 15% Na_2SO_3 was the most amorphous, with high conductivity, ductility, and stability. The tensile strength of SPE decreases with the addition of salt when Na_2SO_3 salt is added becomes 7.033 MPa, but its elongation value increases achieve 792.1%. The effect of adding salt to SPE reduces the samples' bulk resistance. The ionic conductivity value progressively rises as the resistance value declines. The 15% PVA-Glycerol-Na_2SO_3 SPE sample had the highest ionic conductivity, measuring 1.05×10^{-4} S cm^{-1} at 70°C.

Acknowledgment

We acknowledge the Universitas Pertamina for providing material characterization assistance through the Mechanical Engineering and Chemical Engineering Department facility under the UPERESEARCH 2022 Research Grant with project number 0333B/UP-R/SK/HK.01/X/2022.

References

[1] Tengku Azirudin, Potensi Tenaga Angin Di Atas Bangunan Bertingkat di Pangkalan Kerinci, Kabupaten Pelalawan Provinsi Riau, 2019

[2] Muhamad Azhar, Solechan Solechan, Retno Saraswati, Putut Suharso, Suhartoyo Suhartoyo, Budi Ispriyarso, The New Renewable Energy Consumption Policy of Rare Earth Metals to Build Indonesia's National Energy Security, *The 1st Sriwijaya International Conference on Environmental Issues 2018 (1st SRICOENV 2018)*, 2018 https://doi.org/10.1051/e3sconf/20186803008

[3] Djoni Hartono, Arief Anshory Yusuf, Sasmita Hastri Hastuti, Novani Karina Saputri, Noor Syaifudin, Effect of COVID-19 on energy consumption and carbon dioxide emissions in Indonesia, *Sustainable Production and Consumption*, 28, (2021), 391-404 https://doi.org/10.1016/j.spc.2021.06.003

[4] Aan Jaelani, Slamet Firdaus, Juju Jumena, Renewable Energy Policy in Indonesia: The Qur'anic Scientific Signals in Islamic Economics Perspective, *International Journal of Energy Economics and Policy*, 7, 4, (2017), 193-204

[5] J. Mitali, S. Dhinakaran, A. A. Mohamad, Energy storage systems: a review, *Energy Storage and Saving*, 1, 3, (2022), 166-216 https://doi.org/10.1016/j.enss.2022.07.002

[6] Harsh Kumar, Kamil Kuča, Shashi Kant Bhatia, Kritika Saini, Ankur Kaushal, Rachna Verma, Tek Chand Bhalla, Dinesh Kumar, Applications of Nanotechnology in Sensor-Based Detection of Foodborne Pathogens, *Sensors*, 20, 7, (2020), 1966 https://doi.org/10.3390/s20071966

[7] Muhammad Syukri Mohamad Misenan, Azwani Sofia Ahmad Khiar, Tarık Eren, Polyurethane-based polymer electrolyte for lithium ion batteries: a review, *Polymer International*, 71, 7, (2022), 751-769 https://doi.org/10.1002/pi.6395

[8] Jayeeta Chattopadhyay, Tara Sankar Pathak, Diogo M. F. Santos, Applications of Polymer Electrolytes in Lithium-Ion Batteries: A Review, *Polymers*, 15, 19, (2023), 3907 https://doi.org/10.3390/polym15193907

[9] Agathe Naboulsi, Ronan Chometon, François Ribot, Giao Nguyen, Odile Fichet, Christel Laberty-Robert, Correlation between Ionic Conductivity and Mechanical Properties of Solid-like PEO-based Polymer Electrolyte, *ACS Applied Materials & Interfaces*, 16, 11, (2024), 13869-13881 https://doi.org/10.1021/acsami.3c19249

[10] D. R. Lu, C. M. Xiao, S. J. Xu, Starch-based completely biodegradable polymer materials, *Express polymer letters*, 3, 6, (2009), 366-375 https://doi.org/10.3144/expresspolymlett.2009.46

[11] Nihed Ben Halima, Poly(vinyl alcohol): review of its promising applications and insights into biodegradation, *RSC Advances*, 6, 46, (2016), 39823-39832 https://doi.org/10.1039/C6RA05742J

[12] M. Ue, Secondary Batteries – Lithium Rechargeable Systems | Electrolytes: Nonaqueous, in: J. Garche (Ed.) *Encyclopedia of Electrochemical Power Sources*, Elsevier, Amsterdam, 2009, https://doi.org/10.1016/B978-044452745-5.00207-0

[13] M. S. M. Misenan, A. S. A. Khiar, Conduction Mechanism of Chitosan/Methylcellulose/1-Butyl-3 Methyl Imidazolium Bis (Trifluoromethylsulfonyl) Imide (BMIMTFSI) Biopolymer Electrolyte Doped with Ammonium Triflate, *Malaysian Journal of Chemistry*, 22, 4, (2020), 1-13

[14] M. S. M. Misenan, A. S. A. Khiar, Optimization of methyl cellulose biopolymer electrolyte conductivity via response surface methodology, *Next Materials*, 3, (2024), 100089 https://doi.org/10.1016/j.nxmate.2023.100089

[15] Xinxin Cai, Zhiyu Hu, Wentao Deng, Hongshuai Hou, Xiaobo Ji, Guoqiang Zou, Insight into the Improvement Strategies of Aqueous Electrolyte for Aqueous Rechargeable Batteries, *Batteries & Supercaps*, 7, 5, (2024), e202300619 https://doi.org/10.1002/batt.202300619

[16] D. B. Kal'nyi, V. V. Kokovkin, I. V. Mironov, Sodium sulfite: A promising reagent in the electrochemical oxidation of metallic silver, *Russian Journal of General Chemistry*, 81, 5, (2011), 793-798 https://doi.org/10.1134/S107036321105001X

[17] Ashish Raj, Kushal Mehrotra, S. P. Pandey, S. Venkatesan Jayakumar, Amit Saxena, Bhaskar Bhattacahrya, Humidity Effect on Ionic Conductivity of Composite Polymer Electrolytes, *Macromolecular Symposia*, 407, 1, (2023), 2100467 https://doi.org/10.1002/masy.202100467

[18] Andrei A. Bunaciu, Vu Dang Hoang, Hassan Y. Aboul-Enein, Applications of FT-IR Spectrophotometry in Cancer Diagnostics, *Critical Reviews in Analytical Chemistry*, 45, 2, (2015), 156-165 https://doi.org/10.1080/10408347.2014.904733

[19] A. C. W. Ong, N. A. Shamsuri, S. N. A. Zaine, Dedikarni Panuh, M. F. Shukur, Nanocomposite polymer electrolytes comprising starch-lithium acetate and titania for all-solid-state supercapacitor, *Ionics*, 27, 2, (2021), 853-865 https://doi.org/10.1007/s11581-020-03856-3

[20] Fatin Farhana Awang, Mohd Faiz Hassan, Khadijah Hilmun Kamarudin, Corn starch doped with sodium iodate as solid polymer electrolytes for energy storage applications, *Acta Polytechnica*, 61, 4, (2021), 497-503 https://doi.org/10.14311/AP.2021.61.0497

[21] S. Shanmuga Priya, M. Karthika, S. Selvasekarapandian, R. Manjuladevi, Preparation and characterization of polymer electrolyte based on biopolymer I-Carrageenan with magnesium nitrate, *Solid State Ionics*, 327, (2018), 136-149 https://doi.org/10.1016/j.ssi.2018.10.031

[22] Yushi Fujita, Yusuke Kawasaki, Takeaki Inaoka, Takuya Kimura, Atsushi Sakuda, Masahiro Tatsumisago, Akitoshi Hayashi, Amorphous Li_2O–LiI Solid Electrolytes Compatible to Li Metal, *Electrochemistry*, 89, 4, (2021), 334-336 https://doi.org/10.5796/electrochemistry.21-00049

[23] Christie L. C. Ellis, Emily Smith, Hamza Javaid, Gabrielle Berns, Dhandapani Venkataraman, Chapter 6 - Ion Migration in Hybrid Perovskites: Evolving Understanding of a Dynamic Phenomenon, in: S. Thomas, A. Thankappan (Eds.) *Perovskite Photovoltaics*, Academic Press, 2018, https://doi.org/10.1016/B978-0-12-812915-9.00006-X

[24] Mohamad Rafi, Widia Citra Anggundari, Tun Tedja Irawadi, Potensi spektroskopi FTIR-ATR dan kemometrik untuk membedakan rambut babi, kambing, dan sapi, *Indonesian journal of chemical science*, 5, 3, (2016), 229-234

[25] Asep Bayu Dani Nandiyanto, Rosi Oktiani, Risti Ragadhita, How to Read and Interpret FTIR Spectroscope of Organic Material, *Indonesian Journal of Science and Technology*, 4, 1, (2019), 97-118 https://doi.org/10.17509/ijost.v4i1.15806

[26] Yichao Wu, Anmin Huang, Shuhong Fan, Yuejun Liu, Xiaochao Liu, Crystal Structure and Mechanical Properties of Uniaxially Stretched PA612/SiO2 Films, *Polymers*, 12, 3, (2020), 711 https://doi.org/10.3390/polym12030711

[27] Ana Carolina Marques, Tomás Pinheiro, Gabriela Vieira Martins, Ana Rita Cardoso, Rodrigo Martins, Maria Goreti Sales, Elvira Fortunato, Chapter Seven - Non-enzymatic lab-on-paper devices for biosensing applications, in: A. Merkoçi (Ed.) *Comprehensive Analytical Chemistry*, Elsevier, 2020, https://doi.org/10.1016/bs.coac.2020.05.001

[28] Dimas Rio Priyambodo, Sintesis dan Karakterisasi Polimer Elektrolit PEO/$NaClO_4$/Fly Ash PT. Tjiwi Kimia Mojokerto Pada Baterai Ion Natrium, Kimia, Institut Teknologi Sepuluh Nopember, 2017

[29] M. N. Hafiza, M. I. N. Isa, Solid polymer electrolyte production from 2-hydroxyethyl cellulose: Effect of ammonium nitrate composition on its structural properties, *Carbohydrate Polymers*, 165, (2017), 123-131 https://doi.org/10.1016/j.carbpol.2017.02.033

[30] N. Farah, H. M. Ng, Arshid Numan, Chiam-Wen Liew, N. A. A. Latip, K. Ramesh, S. Ramesh, Solid polymer electrolytes based on poly(vinyl alcohol) incorporated with sodium salt and ionic liquid for electrical double layer capacitor, *Materials Science and Engineering: B*, 251, (2019), 114468 https://doi.org/10.1016/j.mseb.2019.114468